| BRIEF PAPER | Special Section on Recent Advances in Simulation Techniques and Their Applications for Electronics |

Analysis of Instantaneous Acoustic Fields Using Fast Inverse Laplace Transform

Seiya KISHIMOTO[†a)], *Member*, **Naoya ISHIKAWA**[†], *Student Member*, *and* **Shinichiro OHNUKI**[†], *Fellow*

SUMMARY   In this study, a computational method is proposed for acoustic field analysis tasks that require lengthy observation times. The acoustic fields at a given observation time are obtained using a fast inverse Laplace transform with a finite-difference complex-frequency-domain. The transient acoustic field can be evaluated at arbitrary sampling intervals by obtaining the instantaneous acoustic field at the desired observation time using the proposed method.

key words: *acoustics, time-domain, finite-difference complex-frequency-domain, fast inverse Laplace transform*

1. Introduction

Simulations of propagating acoustic fields are useful for hall design, room acoustics, and sound source design [1]–[7]. It is important to evaluate the transition of sound propagation from low to high frequencies based on the spatial distribution of the sound pressure. As the audible range of the human ear is 20–20,000 Hz, the simulation of audible sound is a broadband problem.

Numerical simulation methods for acoustic fields include the finite element method, the boundary element method, the finite-difference time-domain (FDTD) method, and geometric acoustics [6]–[11]. The FDTD method, which was developed for electromagnetic field analysis, can be used to analyze time evolution problems from the perspective of wave acoustics [1], [6]–[8]. However, when the FDTD method is used to analyze time responses, the maximum stable time step size is limited by the propagation speed of the wave in the medium and the minimum size of the spatial discrete section [8]. Moreover, the evaluation of resonators with high Q values and the reverberation time for hall design requires observation of time responses over a long period. This inevitably increases the number of field updates.

In this study, a computational method for acoustic problems is proposed that can be used to observe sound pressure distributions over any specified duration. To this end, the governing equations of the sound field are extended to the complex-frequency domain and solved using the finite-difference complex-frequency-domain (FDCFD) method [12]. Then, the time-domain solution is obtained using the fast inverse Laplace transform (FILT) method [13]–[16]. FDCFD-FILT is applied to solve acoustic problems for the first time by this study. The transient acoustic field can be evaluated at arbitrary sampling intervals by estimating the instantaneous acoustic field at the desired observation time using the proposed method. Further, time-division complete parallel computing can be realized, and the computational task can be temporally divided without the requirement of data communication. Thus, the proposed method is suitable for acoustic field analysis, which often involves long observation times.

2. Computational Method

In this section, the proposed computational method to analyze acoustic fields in the time domain is described by combining a complex-frequency domain solver with the FILT.

2.1 Fast Inverse Laplace Transform

FILT is a computational method used to numerically perform the inverse Laplace transform [13]–[16]. The Bromwich integral replaces the finite series for numerical computations. In this method, the nth sampling complex frequency, s_n, required for the inverse transform can be determined from the poles of the approximated exponential function. The acoustic fields in the complex-frequency domain, $F(s)$, can be transformed into the time domain using the following equations:

$$f(t) = \frac{e^\alpha}{t} \left(\sum_{n=1}^{K} F_n + \frac{1}{A_{q0}} \sum_{m=1}^{q} A_{qm} F_{K+m} \right) \tag{1}$$

$$F_n = (-1)^n \text{Im}[F(s_n)] \tag{2}$$

$$s_n = \frac{\alpha + i(n - 0.5)\pi}{t} \tag{3}$$

$$A_{qq} = 1, A_{q0} = 2^q,$$

$$A_{qm} = A_{qm-1} - \frac{(q + 1)!}{m!(q + 1 - m)!} \tag{4}$$

Here, $f(t)$ is the acoustic field in the time domain, α is the approximation parameter of the exponential function, K is the truncation number, and q is the number of terms in the Euler transformation. In FILT, the acoustic fields at an observation time, t, are obtained by calculating a function in the complex-frequency domain. The second term of (1) is the Euler transformation used to achieve rapid convergence of the alternating series.
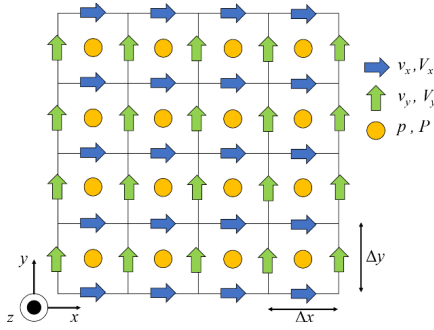
Fig. 1 Yee grid for finite difference scheme for space discretization. Δx and Δy are the segmented areas. The particle velocity vector and the sound pressure are discretized by half-cell displacement.

2.2 Finite-Difference Complex-Frequency-Domain

The governing equations for the analysis of the acoustic fields in the time domain are as follows:

$$\rho \frac{\partial v(r,t)}{\partial t} = -\nabla p(r,t) \tag{5}$$

$$\frac{\partial p(r,t)}{\partial t} = -\rho c^2 \nabla \cdot v(r,t) + p_{in}(r,t) \tag{6}$$

where ρ is the density, v is the particle velocity vector in the time domain, r is the position vector, p is the sound pressure in the time domain, c is the sound velocity in the medium, and $p_{in}(r,t)$ is the source of the incident wave. In the conventional FDTD, the particle velocity vector and sound pressure are discretized using Yee cells, as shown in Fig. 1 [1], [6]–[8]. The temporal and spatial derivatives in (5) and (6) are replaced with finite differences. The sound pressure, p^n, and the particle velocity vector, v^n, are updated using the sound pressure, p^{n-1}, and particle velocity vector, v^{n-1} of the previous time step.

To consider the complex-frequency domain, the Laplace transform is applied to (5) and (6) to obtain the following equations [17], [18]:

$$\rho s V(r,s) - \rho v(r,0) = -\nabla P(r,s) \tag{7}$$

$$s P(r,s) - p(r,0) = -\rho c^2 \nabla \cdot V(r,s) + P_{in}(r,s) \tag{8}$$

where V is the particle velocity vector in the complex-frequency domain, P is the sound pressure in the complex-frequency domain, and P_{in} is the image function of the incident wave in the complex-frequency domain. To solve (7) and (8), the particle velocity vector and sound pressure are discretized using the Yee grid used for FDTD, i.e., the one shown in Fig. 1. The central difference is applied using the following equation.

$$\rho s V_x(x,y) + \frac{P(x+0.5\Delta x, y) - P(x-0.5\Delta x, y)}{\Delta x}$$
$$= \rho v_x(x,y,0) \tag{9}$$

$$\rho s V_y(x,y) + \frac{P(x,y+0.5\Delta x) - P(x,y-0.5\Delta y)}{\Delta y}$$
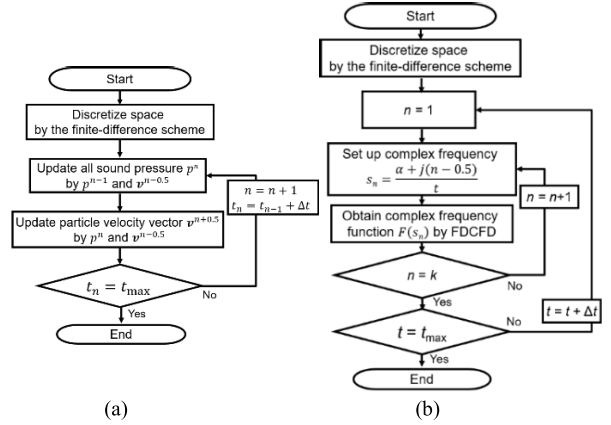$$= \rho v_y(x,y,0) \tag{10}$$

Fig. 2 Flowchart for analysis of time response using (a) FDTD and (b) FDCFD-FILT. In FDTD, the time evolution of the sound fields is determined via sequential calculations based on the information of the previous time step. FDCFD-FILT can compute the instantaneous value of the observation time t from a function in the complex-frequency domain.

$$s P(x,y) + \rho c^2 \left(\frac{V_x(x+0.5\Delta x, y) - V_x(x-0.5\Delta x, y)}{\Delta x} \right.$$
$$\left. + \frac{V_y(x, y+0.5\Delta y) - V_y(x, y-0.5\Delta x)}{\Delta y} \right)$$
$$= p(x,y,0) \tag{11}$$

where Δx and Δy represent the segmented areas. By applying (9)–(11) to the entire analysis space, a linear equation can be obtained. The particle velocity vector and sound pressure in the complex-frequency domain can then be obtained by solving that linear equation: These complex-frequency functions can be transformed into the time domain by using the FILT given in (1).

Figure 2 (a) and (b) depict flowcharts for time-response analysis using FDTD and the proposed method, respectively. In FDTD, the time evolution is determined using a sequential calculation based on the information of the previous time step. Here, the time step size, Δt, of the FDTD is limited by the sound velocity, c, in the medium and Δx and Δy in space, as follows:

$$\Delta t \leq \left(c \sqrt{(\Delta x)^{-2} + (\Delta y)^{-2}} \right)^{-1} \tag{12}$$

In contrast, the proposed method is capable of computing the instantaneous value at any observation time, t, using a function in the complex-frequency domain. As this computation does not require information from previous time steps, it does not impose any restriction on the selected time step size.

3. Computational Results

Figure 3 shows a computational model of the acoustic scattering problem. The scatterer is assumed to be a cylinder with radius $a = 0.5$ m and consists of acoustic soft media, where the sound pressure, p, is equal to 0 at the surface. When the scatterer is a cylinder, a rigorous solution can be
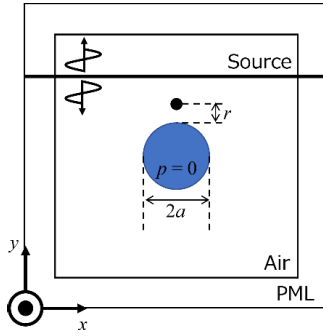
Fig. 3 Computational model for validation of the proposed method. The scatterer is a cylinder of radius a and consists of acoustic soft medium ($p = 0$ at the boundary).

(a)

(b)

Fig. 4 Sound pressure distribution over the computational area. (a) FDTD and (b) FDCFD-FILT. Observation time $t = 0.0135$ s. FDCFD-FILT can compute the sound field at specific observation time.

mathematically obtained, as in the case of electromagnetic scattering problems [14]. An observation point is set 0.5 m from the surface of the cylinder along the $+y$ axis. The wave source is a continuous plane wave with a frequency, $f = 440$ Hz, which is incident from a surface 2 m from the center of the cylinder. The segmentation area, Δx, is set to 0.02 m, which is 1/50th of the diameter of the cylinder. For the scattering analysis, the computational area is covered by a perfectly matched layer (PML) [19], [20]. In this problem, the FDCFD-FILT can be used to obtain the sound pressure distribution at an arbitrary time. Furthermore, to validate the acoustic field analysis performance of FDCFD-FILT, we compared the computational results of FDTD and the exact solution with our results.

The sound field distributions obtained using FDTD and FDCFD-FILT are shown in Figs. 4 (a) and (b), respectively. The observation time was set as $t = 0.0135$ s. In both results, the sound waves were scattered by the cylinder and reduced in the shadowed area. As information of previous time steps is required in the FDTD method to update the sound pressure, a sequential calculation is necessary to obtain the sound field distribution at a specific observation time. In contrast, the sound pressure distribution at any given observation time can be obtained using FDCFD-FILT without any such calculation.

Figure 5 illustrates the time responses of the sound pressure at the observation point. The dots represent the computational results obtained using the FDCFD-FILT method. The blue solid line and the red dashed line represent the exact solution and the FDTD results, respectively. All results are observed to be in good agreement. The circles and triangles indicate the time-step sizes of $\Delta t = 1/20f$ and $\Delta t = 1/2f$, respectively, where f denotes the frequency of the incident wave. As instantaneous values can be computed using our method, time steps of an arbitrary size can be selected to calculate the time responses.

To verify the computational accuracy of the proposed method, the convergence of FILT for varying truncation numbers, K, in (1) was confirmed. The relative error between the exact solution and the results obtained using the proposed method is shown in Fig. 6. The observation time
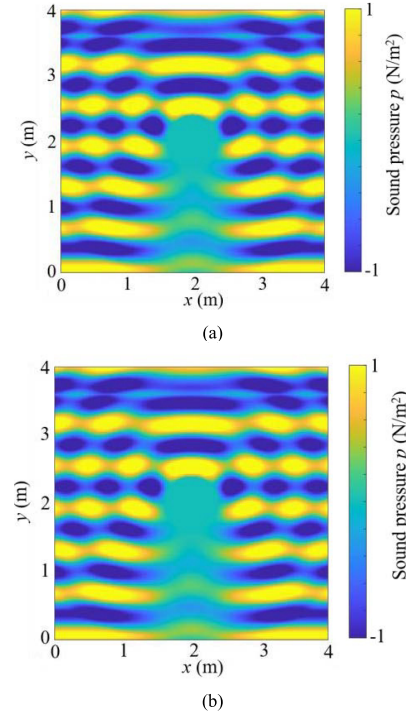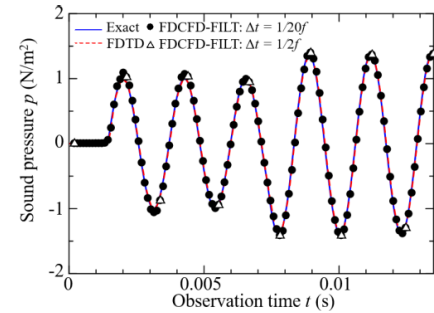

Fig. 5 Time response of sound pressure at the observation point. The exact solution, FDTD results, and results obtained using the proposed method are in agreements. Arbitrary time step size can be selected in the proposed method.

was set to $t = 0.0135$ s, where the sum of the incident and scattered waves is the peak in Fig. 5. The number of terms in the Euler transform was $q = 18$. The relative error converged as the truncation number increased. Moreover, the digits of the convergence value and the approximation parameter α were consistent. This establishes the capability of the proposed method to control errors.

In terms of computational efficiency, unlike FDTD, time-division complete parallel computing can be achieved using FDCFD-FILT. After determining the time evolution of the acoustic field, the instantaneous field computation for each observation time can be distributed into independent computational processes. Table 1 enumerates the speed up rates achieved using parallel computing. The speed up rate
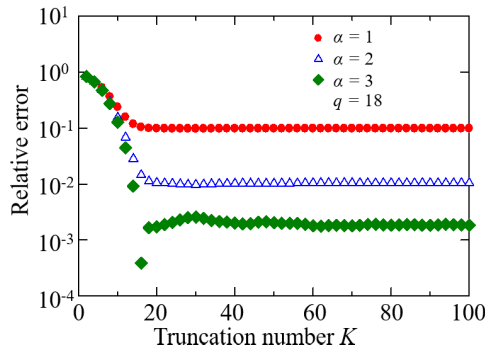
Fig. 6 Convergence test of FILT for varying values of truncation number, K. The relative error converges with increasing truncation number, K. The digits of the convergence value are consistent with the approximation parameter, a.

Table 1 Speed up rate using time-division parallel computing.

Number of computers	Speed up rate
1	1
2	1.9951
5	4.9946
10	9.9072

corresponds to the number of computers.

4. Conclusions

In this paper, a time-domain analysis method is discussed for audible sound field analysis that require lengthy observation times. By combining FILT and FDCFD, the proposed method can be used to obtain the sound field distribution at any given observation time. To verify its reliability, the results obtained using this method were compared with the exact solutions and the FDTD results. The computational accuracy of the proposed method was verified by confirming the convergence process when the number of truncations was varied. The time responses could be evaluated using arbitrary sampling points, which validated the computational efficiency of the proposed method. Further, time-division parallel computing could be achieved using the proposed method by temporally dividing the computational task without data communication.

Acknowledgments

References

[1] S. Sakamoto, H. Nagatomo, A. Ushiyama, and H. Tachibana, "Calculation of impulse responses and acoustic parameters in a hall by the finite-difference time-domain method," Acoust. Sci. Technol., vol.29, no.4, pp.256–265, 2008. doi: 10.1250/ast.29.256

[2] A. Osumi, K. Yamada, Y. Asada, and Y. Ito, "Harmonic imaging of a defect in a flat plate using a guided wave generated by a high-intensity aerial ultrasonic wave," Jpn. J. Appl. Phys., vol.58, no.SG, pp.SGGB14-1–8, 2019. doi: 10.7567/1347-4065/ab1a31

[3] R. Nakayama, T. Asami, and H. Miura, "Deformation and impregnation of droplets containing abrasive grains using intense aerial ultrasonic waves," Jpn. J. Appl. Phys., vol.57, no.7S1, pp.07LE13-1–7, 2018. doi: 10.7567/JJAP.57.07LE13

[4] M. Nakazawa and A. Nishikata, "Development of sound localization system with tube earphone using human head model with ear canal," IEICE Trans. Fundamentals, vol.E88-A, no.12, pp.3584–3592, 2005. doi: 10.1093/ietfec/e88-a.12.3584

[5] T. Yokota, S. Sakamoto, and H. Tachibana, "Visualization of sound propagation and scattering in rooms," Acoust. Sci. Technol., vol.23, no.1, pp.40–46, 2002. doi: 10.1250/ast.23.40

[6] S. Bilbao, "Optimized FDTD schemes for 3-D acoustic wave propagation," IEEE/ACM Trans. Audio, Speech, Language Process., vol.20, no.5, pp.1658–1663, 2012. doi: 10.1109/TASL.2012.2186806

[7] K. Kowalczyk and M.V. Walstijn, "Room acoustics simulation using 3-D compact explicit FDTD schemes," IEEE Trans. Audio Speech Lang. Process., vol.19, pp.34–46, 2011. doi: 10.1109/TASL.2010.2045179

[8] A. Taflove and S.C. Hagnes, Computational Electrodynamics The Finite-Difference Time-Domain Method, Boston, MA, USA; Artech House, 2005.

[9] L. Savioja and U.P. Svensson, "Overview of geometrical room acoustic modeling techniques," J. Acoust. Soc. Am., vol.138, no.2, pp.708–730, 2015. doi: 10.1121/1.4926438

[10] N.A. Gumerov and R. Duraiswami, "Fast multipole accelerated boundary element methods for room acoustics," J. Acoust. Soc. Am., vol.150, no.3, pp.1707–1720, 2021. doi: 10.1121/10.0006102

[11] L.L. Thompson, "A review of finite-element methods for time-harmonic acoustics," J. Acoust. Soc. Am., vol.119, no.3, pp.1315–1330, 2006. doi: doi.org/10.1121/1.2164987

[12] D. Wu, R. Ohnishi, R. Uemura, T. Yamaguchi, and S. Ohnuki, "Finite-difference complex-frequency-domain method for optical and Plasmonic Analyses," IEEE Photonics Technology Letters, vol.30, no.11, pp.1024–1027, 2018. doi: 10.1109/LPT.2018.2828167

[13] T. Hosono, "Numerical inversion of Laplace transform and some applications to wave optics," Radio Science, vol.16, no.6, pp.1015–1019, 1981. doi: 10.1029/RS016i006p01015

[14] S. Masuda, S. Kishimoto, and S. Ohnuki, "Reference solutions for time domain electromagnetic solvers," IEEE Access, vol.8, no.1, pp.44318–44324, 2020. doi: 10.1109/ACCESS.2020.2977382

[15] S. Kishimoto, S. Nishino, and S. Ohnuki, "Novel computational technique for time-dependent heat transfer analysis using fast inverse Laplace transform," Progress In Electromagnetic Research M, vol.99, pp.45–55, 2021. doi: 10.2528/PIERM20100203

[16] D. Wu, S. Kishimoto, and S. Ohnuki, "Optimal parallel algorithm of fast inverse Laplace transform for electromagnetic analyses," IEEE Antennas and Wireless Propagation Letters, vol.19, no.12, pp.2018–2022, 2020. doi: 10.1109/LAWP.2020.3020327

[17] R.D. Strum and J.R. Ward, Laplace transform solution of differential equations, NJ, USA: Pearson Education, 1968.

[18] F. Oberhettinger and L. Badii, Tables of Laplace transform, Berlin, Germany: Springer.

[19] J.-P. Berenger, "A perfectly matched layer for the absorption of electromagnetic waves," J. Compute. Phys., vol.114, no.2, pp.185–200, 1994. doi: 10.1006/jcph.1994.1159

[20] Y. Xiaojuen, D. Borup, J.W. Wiskin, M. Berggren, R. Eidens, and S.A. Johnson, "Formulation and validation of Berenger's PML absorbing boundary for the FDTD simulation of acoustic scattering," IEEE Trans. Ultrason. Ferroelectr. Freq. Control, vol.44, no.4, pp.816–822, 1997. doi: 10.1109/58.655197